ACTA ABP BIOCHIMICA POLONICA

Vol. 70, No 1/2023
153–162
https://doi.org/10.18388/abp.2020_6379

Regular paper

Circular RNA LPAR3 targets JPT1 *via* microRNA-513b-5p to facilitate glycolytic activation but repress prostate cancer radiosensitivity

Yuan Yuan Chen[1], Li Ping Luo[1]✉ and Ke Chong Deng[2]✉

[1]Department of Oncology, Wuhan Wuchang Hospital Affiliated to Wuhan University of Science and Technology, Wuhan City, Hubei Province, 430063, China; [2]Department of Emergency, Wuhan Wuchang Hospital Affiliated to Wuhan University of Science and Technology, Wuhan City, Hubei Province, 430063, China

A great many circular RNAs (circRNAs) are considered key modulators of human malignancies. However, the function of circRNA lysophosphatidic acid receptor 3 (LPAR3) in the radioresistance of prostate cancer (PCa) cells is still uncertain. circLPAR3, microRNA (miR)-329-3p, and JPT1 expression in PCa tissues and cells were detected by real-time quantitative PCR or western blot. Cell proliferation was detected by CCK-8 (cell proliferation assay) and colony formation assay, apoptosis was by flow cytometry, and migration and invasion ability were by Transwell assay. Cell glycolysis was analyzed by glucose uptake, lactate production, and ATP metabolism. Under different doses of radiation, the radiosensitivity of PCa cells was detected by colony formation assay. The relationship between circLPAR3, miR-513b-5p, and JPT1 was confirmed by dual luciferase reporter gene detection and RIP assay. The data presented that circLPAR3 and JPT1 expression was elevated in PCa, while miR-513b-5p expression was reduced. Repression of circLPAR3 depressed cell advancement, and restrained glycolysis, but enhanced the radiosensitivity of PCa cells. CircLPAR3's target miRNA was miR-513b-5p which targeted JPT1. Elevated JPT1 reversed the repressive effects of circLPAR3 knockdown or miR-513b-5p overexpression on PCa advancement, glycolysis, and radiosensitivity. In summary, the knockdown of circLPAR3 reduces glycolysis, but promotes PCa radiosensitivity *via* the miR-513b-5p/JPT1 axis, discovering a novel mechanism in PCa progression.

Keywords: prostate cancer, circular RNA lysophosphatidic acid receptor 3, MicroRNA-513b-5p, Jupiter microtubule associated homolog 1, glycolysis, radiosensitivity

Received: 31 May, 2022; revised: 09 October, 2022; accepted: 29 January, 2023; available on-line: 17 March, 2023

✉e-mail: 1329195378@qq.com (LPL); 65490595@qq.com (KCD)
Abbreviations: circRNA, circular RNA; JPT1, Jupiter microtubule associated homolog 1; LC, lung cancer; LPAR3, lysophosphatidic acid receptor; miRNAs, MicroRNAs; PCa, prostate cancer

INTRODUCTION

Prostate cancer (PCa) is a common cancer among men worldwide, and its mortality rate ranks 2nd among men's cancers (Wu *et al*., 2019). Recently, the incidence rate of PCa in China has manifested an upward trend (Zhou *et al*., 2021). In addition to surgical resection, radiotherapy is another treatment approach that can cure PCa (Li *et al*., 2020). Nevertheless, owing to radioresistance, the effectiveness of radiotherapy is unsatisfactory. Therefore, it is vital to explore a way to promote radiosensitivity.

Circular RNA (circRNA) is an endogenous non-coding RNA transcribed by RNA polymerase II, and featured by linking the 3' with 5' ends *via* exon or intron cycles (Kong *et al*., 2017). Studies have clarified that circRNA is crucial in various biological processes like apoptosis, cell vascularization, and cell invasion (Yuan *et al*., 2019). For instance, circRNA La-related RNA-binding protein 4 (LARP4) represses cell migration and invasion of PCa *via* targeting FOXO3A (Weng *et al*., 2020).. circRNA is differentially manifested in cancers and could serve as a latent modulator of tumorigenesis or cancer advancement. For instance, circ-membrane bound O-acyltransferase domain containing 2 accelerates PCa advancement *via* the miR-1271-5p/mTOR axis (Shi *et al*., 2020). CircRNA lysophosphatidic acid receptor 3 (LPAR3), a novel circRNA discovered recently, has been testified to be aberrantly manifested in several human cancers, like esophageal cancer (Shi *et al*., 2020) and ovarian cancer (Xu *et al*., 2020). However, its expression and function in PCa are not yet distinct.

MicroRNAs (miRNAs) are a set of short endogenous non-coding RNAs that could control approximately 30–50% of human protein-coding genes and molecular signaling pathways in cells (Porzycki *et al*., 2018). Accumulating evidence clarify that miRNAs are differentially expressed in cancers and impact cell growth, differentiation and apoptosis processes (Ghafouri-Fard *et al*., 2020). miRNA expression has become a latent biomarker for PCa diagnosis and prognosis (Nayak *et al*., 2020). For instance, miR-424/572 in recurrent PCa specimens are novel biomarkers for predicting PCa progression (Suer *et al*., 2019). MiR-215-5p reduces the metastasis of PCa *via* targeting phosphoglycerate kinase 1 (Chen *et al*., 2020). MiR-513b-5p is dysregulated in multiple human cancers, like lung cancer (LC) (Cai *et al*., 2020), hepatocellular carcinoma (Jin *et al*., 2021) and breast cancer (Lin *et al*., 2020). However, no research is presented to manifest what effects miR-513b-5p has on PCa.

In this study, we discovered the expression of circLPAR3 was more highly expressed in PCa samples than in controls. Therefore, we knock down circLPAR3 expression to identify its potential roles and explore possible mechanisms in carcinogenesis of PCa. Here, we demonstrated that circLPAR3 acted as a miR-513b-5p sponge to up-regulated Jupiter microtubule associated homolog 1 (JPT1). The research suggests that a novel circRNA may serve as a new biomarker for the early diagnosis and treatment of PCa.

MATERIALS AND METHODS

Sample collection

Tumors and normal tissues adjacent to cancer were harvested from 58 patients with PCa in The Affiliated Hospital of Jiaxing University and stored in liquid nitrogen. Approval of this study was obtained from the Ethics Committee of The Affiliated Hospital of Jiaxing University and written informed consent was gained from each patient (Approval number: JX20156211).

Cell culture

PCa cell lines PC-3, LNCaP, VCaP, DU145 and human normal prostate epithelial cell line RWPE-1 were purchased from ATCC (MA, USA). PC3 cells were cultured in FK12 medium (Gibco, CA, USA), LNCaP cells were in RPMI-1640 medium (Gibco), VCaP cells were in 90% Dulbecco's modified Eagle's medium (Gibco), DU145 cells were in Eagle's Minimum Essential Medium; and RWPE-1 cells were in Keratinocyte Serum-Free Medium Kit (Invitrogen, CA, USA). The mediums for PC cell culture were supplemented with 10% fetal bovine serum (Gibco).

Cell transfection

For the inhibition of circLPAR3 and JPT1, shRNA sequences targeting circLPAR3 and JPT1-specific siRNA (si-JPT1) sequences were synthesized by GenePharma. For miRNA overexpression, miR-513b-5p mimic was obtained from GenePharma. Gene overexpression vector (pcDNA-JPT1) and control vector (pcDNA) were purchased from Nanjing Jinrui Biotechnology Co., Ltd. After 24 h of cell culture, plasmids were transfected using Lipofectamine 3000 Transfection Reagent (Invitrogen).

RNase R treatment test

RNase R (6 units, Geneseed Biotech) was added to every 2 g RNA. After RNase R treatment, reverse transcription-quantitative polymerase chain reaction (RT-qPCR) was applied to detect circLPAR3 and LPAR3 in LNCaP cells PMID: 34913472.

Actinomycin D test

The actinomycin D test was performed with LNCaP cells incubated with actinomycin D (2 mg/mL; Sigma-Aldrich, Tokyo, Japan) for 0, 4, 8, 12 and 24 h PMID: 34913472.

Cell counting kit (CCK-8) assay

About 3×10^3 cells were seeded in each well of a 96-well plate and detected proliferation at 24, 48 and 72 hours by CCK-8 (Dojindo, Haidian, Beijing, China). The absorbance at 450 nm was recorded at each time point, and the cell proliferation curve was drawn.

X-ray exposure

X-ray generator (Varian, Palo Alto, CA, USA) was applied to radiation management at a fixed rate of 4 Gy/min.

Colony formation and survival analysis

Approximately 140 transfected cells were incubated in each well of a 6-well plate for 14 to 21 days. Then the staining with 0.5% crystal violet (Yeasen) was observed under an inverted microscope (×40; Leica, Germany). For survival analysis, 200 cells were seeded on a 6-well plate and irradiated at 0, 2, 4, 6, and 8 Gy X-ray or not. Subsequently, a colony formation test was performed as described above.

Flow cytometry

Cells were treated with double-staining with fluorescein isothiocyanate-labeled annexin V (Invitrogen) and propidium iodide and then detected on a FACS Calibur flow cytometer (Becton Dickinson, San Jose, CA, USA) equipped with Cell Quest software (Becton, Franklin Lakes, NJ, USA) PMID: 31733095.

Migration and invasion test

A 24-well transwell chamber (Millipore, Billerica, MA, USA) with an 8 μm polycarbonate membrane was used to perform migration tests on LNCaP cells. Briefly, LNCaP cells (5×10^5 cells/well) were added into the upper chamber with 200 μL of serum-free medium, and the complete medium was added into the lower chamber as a chemoattractant. After 24 h, the migrating submembrane cells were fixed with 95% ethanol for staining with crystal violet (Beyotime, Shanghai, China) and imaging under the microscope (Leica). Image Lab software 5.2 (Bio-Rad, Hercules, CA, USA) was used for data analysis. The 24-well transwell was pre-covered with Matrigel (BD Biosciences) and was needed for invasion detection PMID: 31387394.

Glucose consumption, lactate production and adenosine triphosphate (ATP) levels

A glucose determination kit (Sigma), lactic acid colorimetric/fluorescence determination kit (BioVision) and CellTiter Glo Luminescent Cell survival Assay (Promega) were put to detect glucose consumption, lactate production and ATP levels (Zheng *et al.*, 2020).

qPCR

Total RNA was isolated from PC tissues and cells using TRIzol (Invitrogen). To measure miRNA expres-

Table 1. Fluorescence quantitative PCR primer sequence

Genes	Forward (5′-3′)	Reverse (5′-3′)
CircLPAR3	GAGTTACCTTGTTTTCTGGACA	TGGAGAAGTGAACATCCTAAG
JPT1	ATAGCTCCCGAGTTTTGCG	TTGGCCCAAGAAGCTTGA
GAPDH	GGGAAGCTCACTGGCATGGCCTTCC	CATGTGGGCCATGAGGTCCACCAC
MiR-513b-5p	GGCCGGGGAGCTGGAGAAGA	TCCATGGAGGGTTGGGGGTTCC
U6	CTCGCTTCGGCAGCACATATATT	ACGCTTCACGAATTTGCGTGGC

sion, RNA was reverse transcribed into cDNA using the TaqMan miRNA Reverse Transcription Kit (Applied Biosystems) and then quantified by real-time PCR using TaqMan Universal PCR Master Mix and TaqMan RNA Detection (Applied Biosystems). To measure circRNA expression, RNA was reverse transcribed into cDNA using PrimeScript RT Reagent (Takara) and then quantified by SYBR Premix Ex Taq (Takara). U6 and glyceraldehyde 3-phosphate dehydrogenase (GAPDH) were used as the internal reference. The $2^{-\Delta\Delta Ct}$ method was put into use to calculate the relative miR-513b-5p and the target gene. RT-qPCR primer sequence was manifested in Table 1 PMID: 34515615.

Western blot analysis

Total protein was extracted from cell lysis buffer (Sangon Biotech), separated on 12% sulfate-polyacrylamide gel, and electroblotted onto a polyvinylidene fluoride membrane (Millipore, Billerica, MA, USA). Using primary antibodies JPT1 (ab126705; 1:1000; Abcam) and glyceraldehyde-3-phosphate dehydrogenase (GAPDH) (ab8245; 1:1000; Abcam), the membrane was incubated overnight. Added with the secondary antibody (1:2000, Promega), the membrane was analyzed by Odyssey Infrared Imaging System (LI-COR, Lincoln, NE, USA) PMID: 31624242.

The luciferase activity assay

Co-transfection of circLPAR3/JPT1-wild/mutant types (WT/MUT), miR-513b-5p mimic or miR-NC was conducted in LNCaP cells (Thermo Fisher Scientific) with Lipofectamine 3000. After 48 h, the relative activity of luciferase was detected *via* the dual Glo luciferase detection system (Promega, Shanghai, China).

RNA binding protein immunoprecipitation (RIP) assay

RNA immunoprecipitation kit (Millipore, Bedford, MA, USA) was carried out for RIP detection. LNCaP cells at a density of 5×10^5 cells/plate were treated with ice-cold radioimmunoprecipitation (RIPA) lysis buffer (Beyotime, Shanghai, China), incubated with protein A/G beads containing Anti-Argonaute 2 (anti-Ago2) or anti-Immunoglobulin G (anti-IgG). circLPAR3, miR-513b-5p and JPT1 were examined by RT-qPCR. N=3 (Du *et al.*, 2020).

Statistical analysis

SPSS 21.0 (SPSS, Inc, Chicago, IL, USA) statistical software was applied to analyze the data. After the Kolmogorov-Smirnov test, the data were normally distributed and manifested as mean ± standard de*via*tion (S.D.). The two-group comparison was conducted *via* *t*-test, while the comparison among multiple groups was *via* one-way analysis of variance (ANOVA), and Fisher's least significant difference *t*-test (LSD-*t*). Enumeration data reported as rate or percentage were compared by chi-square test. *P* was a two-sided test; $P<0.05$ emphasized obvious statistical meaning.

RESULTS

We aimed to investigate circLPAR3 expression in PCa and its underlying molecular mechanism of regulating PCa progression by targeting JPT1 through miR-513b-5p. By collecting PCa clinical specimens and culturing PCa cells *in vitro*, we determined the relative expression levels of circLPAR3, miR-513b-5p and JPT1, and further verified their targeting relationship and interaction relationship. Our experiments found that circLPAR3 promoted glycolytic activation by targeting JPT1 through miR-513b-5p and inhibited PCa radiosensitivity. Therefore, our data are the first to investigate the function and mechanism of circLPAR3 in PCa, providing new insights into the pathogenesis of PCa.

Elevated circLPAR3 suggests an unpleasing into bad for PCa patients

CircRNAs are considered to be a promising marker for cancer diagnosis and prognosis. It has been report-

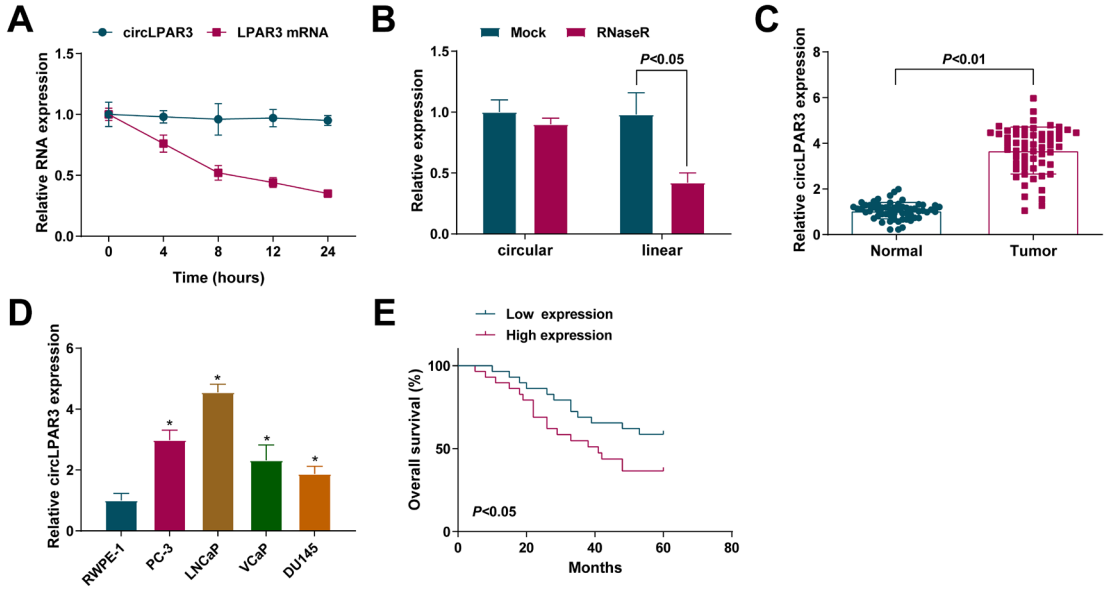

Figure 1. Upregulated circLPAR3 suggests an unpleasing prognosis for PCa patients
(**A**) Actinomycin D and (**B**) circLPAR3 expression after RNase R. G treatment; (**C**) RT-PCR to detect circLPAR3 in PCa specimens vs. normal specimens, n=58. (**D**) RT-PCR to examine circLPAR3 in human normal prostate epithelial cell lines RWPE-1 and PCa cells (PC-3, LNCaP, VCaP, DU145). (**E**) The survival analysis calculated by the Kaplan Meier plotter manifested the survival rate of PCa patients with elevated or reduced circLPAR3, n=58. N=3; The data in the figure were all measurement data, the manifestation of which was as mean ± S.D. **vs.* RWPE-1 cells, $P<0.05$.

Table 2. Correlation between circLPAR3 expression and clinicopathologic characteristics of PCa patients in cohort

Characteristics	Patient frequency (%)	circLPAR3 expression level		*p*-value[a]
		Low	High	
Total cases	58	29	29	
Age				0.424
<65	24	10	14	
≥65	34	19	15	
PSA level (μg/L)				0.585
≤10	21	9	12	
>10	37	20	17	
Gleason score				0.031*
≤7	35	22	13	
>7	23	7	16	
Pathologic stage				0.021*
T1-2	46	27	19	
T3-4	12	2	10	
Lymph-node status				0.279
Negative	39	22	17	
Positive	19	8	12	
Distant metastasis				0.016*
No	34	22	12	
Yes	24	7	17	

Abbreviations: [a]Chi-square test, *P<0.05.

ed that circLPAR3 promotes the migration, invasion and metastasis of esophageal cancer PMID: 32495982. However, the role of circLPAR3 in PCa is still unclear. We first explored the properties of circLPAR3: actinomycin D (Fig. 1A) and RNase R experiments (Fig. 1B) manifested that circLPAR3 was much larger than the linear transcript. circLPAR3 expression in PCa patient specimens was clearly elevated (Fig. 1C). In PCa cell lines, it was discovered that circLPAR3 in PCa cells was enhanced (Fig. 1D). Subsequently, we divided circLPAR3 into high expression and low expression according to the median expression level of circLPAR3 in clinical patients, and analyzed the clinicopathological characteristics of PCa patients, and found that circLPAR3 expression was associated with high Gleason score, advanced pathological T stage and distant metastases (Table 2). The survival analysis calculated by Kaplan Meier affirmed that PCa patients with elevated circLPAR3 had a lower survival rate than those with reduced circLPAR3 (Fig. 1E). All in all, the results affirmed that circLPAR3 suggested an unpleasing prognosis for PCa patients.

Silenced circLPAR3 weakens cell advancement and glycolysis, but enhances radiosensitivity

In order to immediately examine the functional role of circLPAR3 in PCa progression, the introduction of sh-circLPAR3 clearly reduced circLPAR3 (Fig. 2A). It was worth noting that knockdown of circLPAR3 repressed cell advancement (Fig. 2B–F). Glycolysis, characterized by enhanced glucose uptake and lactate accumulation, is a common feature of cancer cells PMID: 34237309. In the meantime, it was manifested that repressingcircLPAR3 restrained glucose uptake, lactate production and ATP levels (Fig. 2G–I). To improve the radiotherapy effect of PCa and improve the radiosensitivity, it is a hot research topic to understand the mechanism of cellular radioresistance PMID: 33033519. It was also determined whether circLPAR3 could impact the radiosensitivity of LNCaP cells *in vitro*. Moreover, with the application of sh-circLPAR3, the cell survival rate was clearly decreased after radiation exposure (Fig. 2J), revealing that circLPAR3 silencing enhanced cell radiosensitivity. The above data clarified silenced circLPAR3 weakened cell advancement with glycolysis but enhanced radiosensitivity *in vitro*.

CircLPAR3 absorbs miR-513b-5p in PCa cells

CircRNAs are involved in the regulation of miR sponges in PCa cells PMID: 34515615. Interestingly, the starBase database predicted a latent binding site between circLPAR3 and miR-513b-5p (Fig. 3A). For verifying whether circLPAR3 could adsorb miR-513b-5p, an experiment was implemented. It was discovered that miR-513b-5p mimic was available to reduce the luciferase activity of the circLPAR3-WT reporter plasmid, while had no clear effect on that of the MUT one (Fig. 3B). Then it was clarified that compared to the control IgG, circLPAR3 and miR-513b-5p were rich in microribonucleoprotein consisting of Ago2 (Fig. 3C). Moreover, reduced miR-513b-5p was detected in PCa (Fig. 3D, E) and was negatively linked with circLPAR3 expression in PCa samples (r=–0.637, Fig. 3F). In cells silencing circLPAR3, miR-513b-5p was found to be up-regulated (Fig. 3G). In general, circLPAR3 adsorbed miR-513b-5p and negatively modulated its levels in PCa cells.

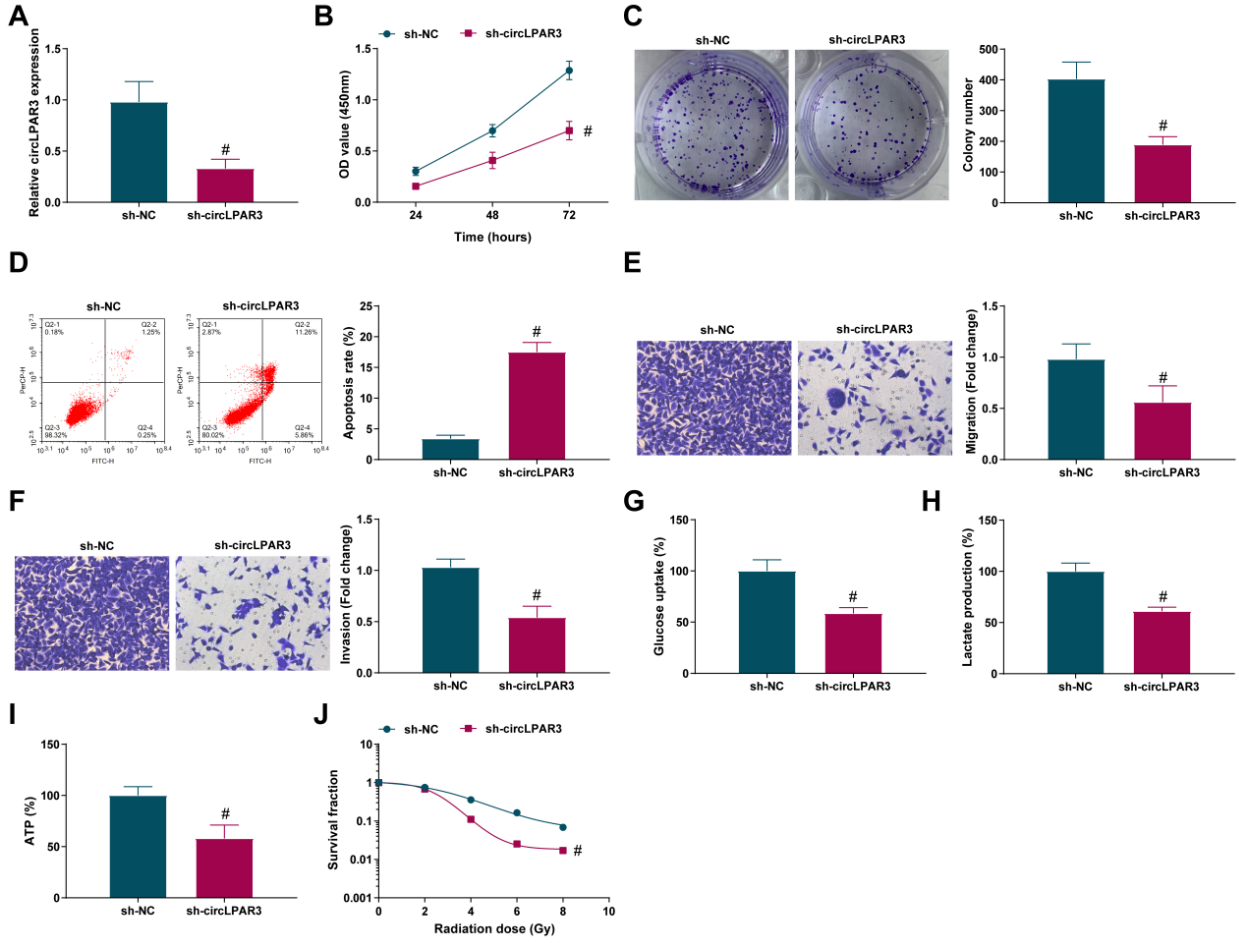

Figure 2. Repressive circLPAR3 weakens cell advancement with glycolysis, but facilitates radiosensitivity *in vitro*
(**A**) circLPAR3-shRNA lentiviral transfection efficiency; (**B**) CCK-8 and (**C**) plate clone to detect cell proliferation ability after repressing circLPAR3; (**D**) Flow cytometry to detect cell apoptosis after depressing circLPAR3; (**E, F**) Transwell detection of cell migration and invasion abilities after restrained circLPAR3; (**G–I**) Glucose uptake, lactate production and ATP metabolism analysis of cell glycolysis; (**J**) Under radiation (0, 2, 4, 6 and 8 Gy) irradiation, colony formation assay to analyze the survival of the transduced cells. N = 3; The data in the figure were all measurement data, the manifestation of which was as mean ± S.D. #*vs*. the sh-NC, $P<0.05$.

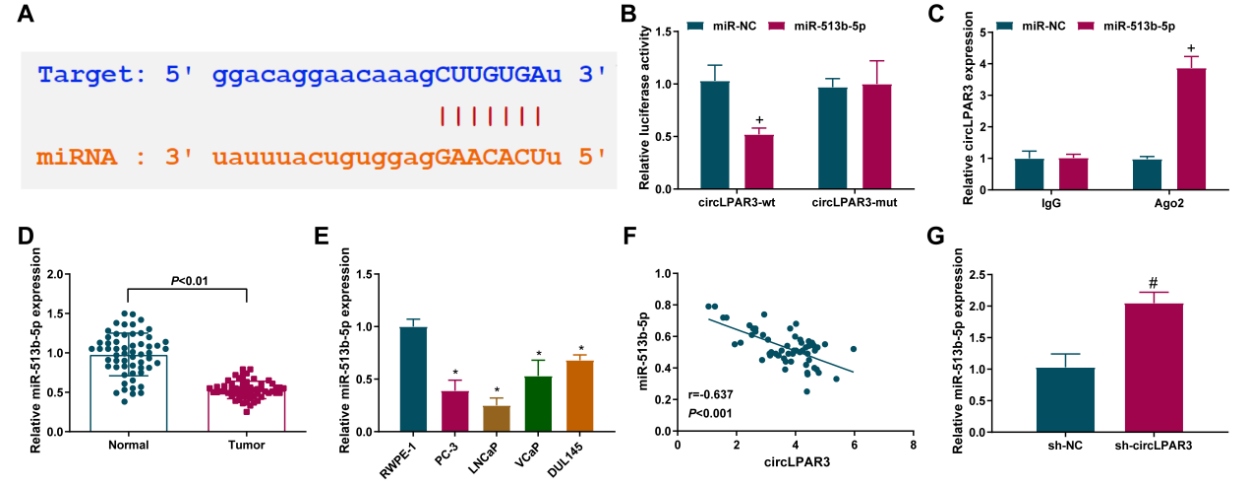

Figure 3. CircLPAR3 absorbs miR-513b-5p in PCa cells
(**A**) Using bioinformatics to predict the latent binding site of circLPAR3 with miR-513b-5p. (**B**) Co-transfection of 293 T cells with WT or MUT circLPAR3 luciferase reporter vector and miR-NC or miR-513b-5p mimic to detect the luciferase activity. (**C**) RIP assay to confirm that circLPAR3 and miR-513b-5p were enriched in micronuclein containing ago2. (**D**) qPCR detection of miR-513b-5p in 58 PCa and normal tissues, n=58; (**E**) qPCR detection of miR-513b-5p in PCa and normal cells; (**F**) Pearson analysis showed circLPAR3 in PCa tissue was negatively linked with miR-513b-5p, n=58. (**G**) Clearly elevated miR-513B-5p in cells with repressive circLPAR3. N=3; The data in the figure were all measurement data, the manifestation of which was as mean ± S.D. +*vs*. the miR-NC, $P<0.05$. **vs*. RWPE-1 cells, $P<0.05$. #*vs*. the sh-NC, $P<0.05$.

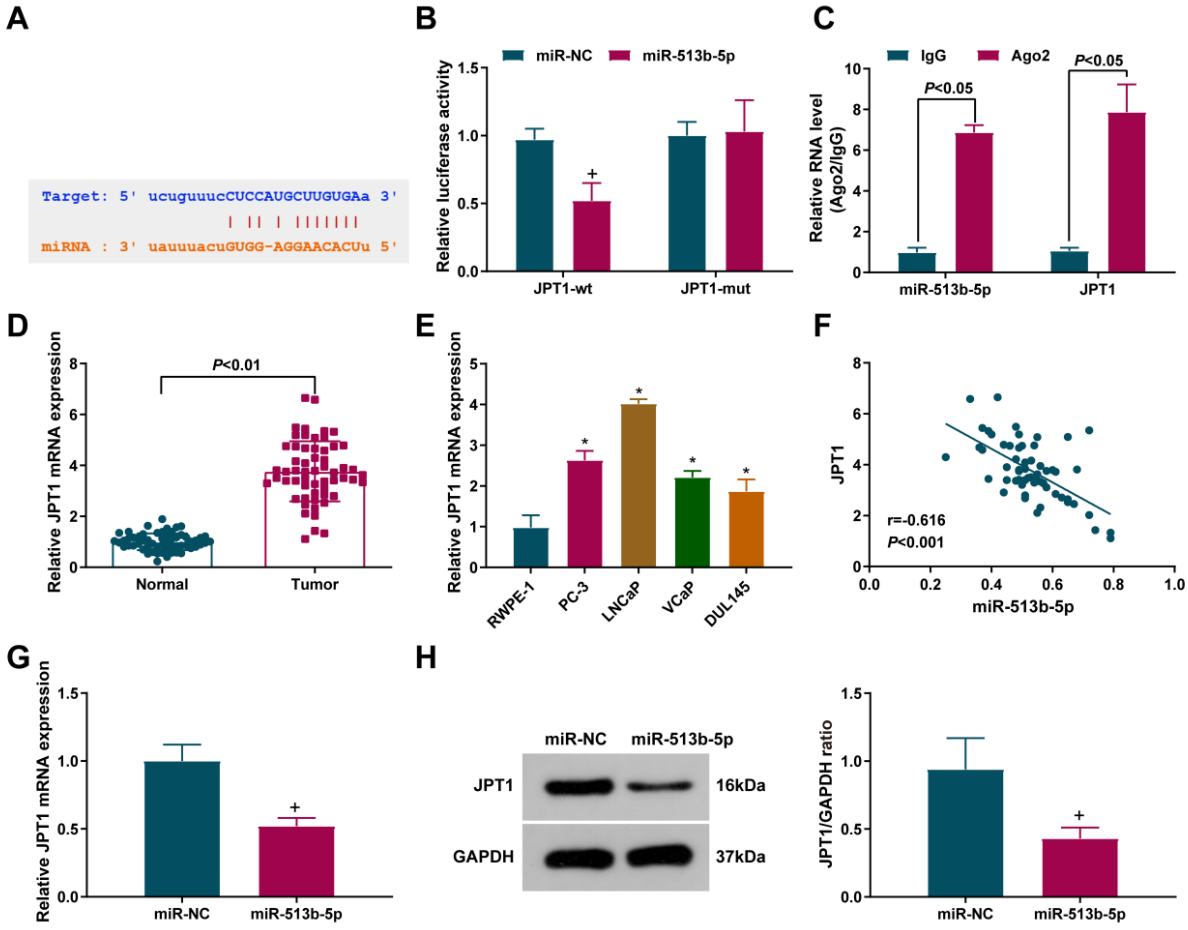

Figure 4. MiR-513b-5p refrains PCa cell growth and glycolysis and promotes cellular radiosensitivity
(**A**) RT-qPCR to detect miR-513b-5p in cells transfected with miR-513b-5p mimic. (**B**) CCK-8 method and (**C**) plate clone to detect PCa cell proliferation after up-regulation of miR-513b-5p. (**D**) Flow cytometry to detect cell apoptosis after elevated miR-513b-5p; (**E, F**) Transwell method to detect the migration and invasion of PCa cells after elevated miR-513b-5p. (**G–I**) Glucose uptake, lactic acid production and ATP metabolism analysis of cellular glycolysis; (**J**) Under different doses of radiation, the survival rate of PCa cells detected by colony formation experiments. N=3; The data in the figure were all measurement data, the manifestation of which was as mean ± S.D. $^{+}$*vs.* the miR-NC, $P<0.05$.

MiR-513b-5p reduces PCa cell growth and glycolysis and promotes cellular radiosensitivity

Altered miRNA expression has been shown to play an important role in PCa invasion and metastasis PMID:34461437, while the expression of miR-513b-5p in PCa is unclear. It was confirmed that miR-513b-5p expression was elevated after miR-513b-5p mimic transfected into LNCaP cells (Fig. 4A). Subsequently, functional test data manifested that up-regulated miR-513b-5p repressed cell progression with glycolysis, but enhanced radiosensitivity *in vitro* (Fig. 4B–J). The above data confirmed that miR-513b-5p restrained growth and glycolysis, and promoted cellular radiosensitivity of PCa cells.

JPT1 is the immediate target of miR-513b-5p

As manifested in Fig. 5A, JPT1 was predicted to be miR-513b-5p's target on StarBase. The miR-513b-5p-transfected JPT1 3'untranslated region (UTR)-WT group produced reduced luciferase activity. At the same time, for verifying whether the predicted binding site of JPT1 with miR-513b-5p was necessary for the two's binding, mutation of the JPT1 binding site was conducted to construct the JPT1 3'UTR-MUT reporter plasmid. When co-transfection with miR-NC/513b-5p, the luciferase activity of the JPT1 3'UTR-MUT group was not impacted (Fig. 5B), suggesting that miR-513b-5p immediately interacted with JPT1. The other experiment also manifested miR-513b-5p was available to combine with JPT1 (Fig. 5C). JPT1 mRNA was clearly up-regulated in cancer tissues and PCa cells than normal tissues adjacent to cancer, and RWPE-1 cells (Fig. 5D, E). It was also discovered that JPT1 and miR-513b-5p were negatively linked (r = -0.616, Fig. 5F). In the meantime, in cells with up-regulated miR-513b-5p, it was found that JPT1 expression was suppressed (Fig. 5G). In summary, miR-513b-5p directly interacted with JPT1 in PCa cells.

Inhibition of JPT1 inhibits cell growth and glycolysis and promotes radiosensitivity *in vitro*

To further examine the functional role of JPT1 in PCa, we knocked down JPT1 in cells (Fig. 6A). Responded to inhibition of JPT1, cell growth and glycolysis were suppressed and radiosensitivity was induced (Fig. 6B–J). Collectively, inhibition of JPT1 inhibits cell growth and glycolysis, and promotes radiosensitivity *in vitro*.

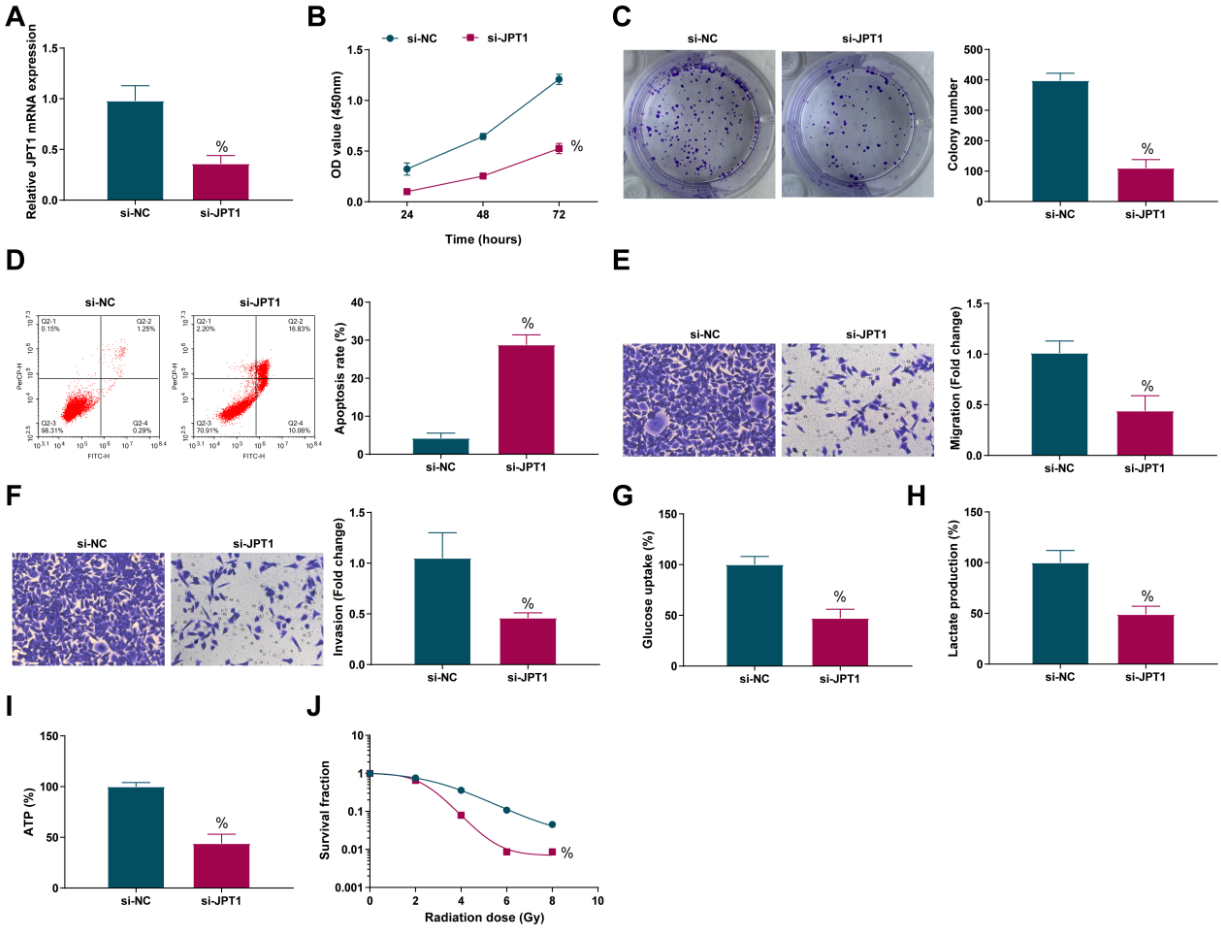

Figure 5. JPT1 is the immediate target of miR-513b-5p
(**A**)Prediction of the binding area between JPT1 and miR-513b-5p using the StarBase database. (**B**) The luciferase activity assay to detect the interaction between miR-513b-5p and JPT1 target protein. (**C**) RIP test to evaluate the binding of miR-513b-5p to JPT1. (**D, E**) RT-qPCR to detect JPT1 mRNA in PCa tissues and cells, n=58. (**F**) Pearson to analyze the linear relationship between miR-513b-5p and JPT1, n=58. (**G, H**) RT-qPCR and Western blot to detect JPT1 in PCa cells after up-regulated miR-513b-5p. N=3; The data in the figure were all measurement data, the manifestation of which was as mean ± S.D. **vs.* RWPE-1 cells, $P<0.05$; +*vs.* the miR-NC, $P<0.05$

Overexpression of JPT1 reversed the role of downregulated circLPAR3 or upregulated miR-513b-5p on cancer cell growth

For determining the influence of miR-513b-5p on PCa development and the possible mechanism, a rescue experiment was conducted by transfection with sh-circLPAR3 + pcDNA-NC, sh-circLPAR3 + JPT1, miR-513b-5p + pcDNA-NC or miR-513b-5p + JPT1 in LNCaP cells (Fig. 7A). The experiment clarified that elevated JPT1 reversed the repressive effects of silenced circLPAR3 or up-regulated miR-513b-5p on PCa advancement with glycolysis, and radiosensitivity (Fig. 7B–J). All in all, overexpression of JPT1 reversed the inhibition of circLPAR3 or upregulated miR-513b-5p on cancer cell growth.

DISCUSSION

At present, PCa has surpassed LC to become the most prevalent malignant tumor in American men. Although the overall survival rate of PCa patients has been improved owing to crucial advances in early screening and cancer management programs, the pathogenesis of PCa is still ambiguous yet (Wang *et al.*, 2019). CircRNA has been proven to be a critical modulator of human cancer, and it can perform its functions *via* cooperating with its host gene (Liu *et al.*, 2020). In this study, it was discovered for the first time that circLPAR3 was elevated in PCa patients, and PCa patients with upregulated circLPAR3 had a lower survival rate. This result suggested circLPAR3 could be applied as a latent biomarker for poor prognosis. Hence, exploring the function of circRNA in PCa can be a breakthrough to understand the pathogenesis of PCa.

A study has clarified that the reprogramming of cell metabolism is closely implicated in tumorigenesis and can be applied to cancer treatment (Xia *et al.*, 2020). Because cancer cells have a strong ability to reproduce, hypoxia frequently shows up during tumor growth (Wang *et al.*, 2019). As we all know, normal cells generally produce energy through mitochondrial oxidative phosphorylation, while quick cancer cell proliferation requires more energy. Therefore, the metabolic pathway of hypoxic cancer cells must be different from the normal metabolic pathway. It is reported that hypoxia facilitates the development of tumor cells to produce the inefficient pathways of ATP, making them inclined to gain energy *via* the glucose-dependent glycolysis pathway, which is necessary to maintain the rapid growth of tumors, also known as the Warburg effect (Dyshlovoy *et al.*, 2020). Hence, repressing the activation of

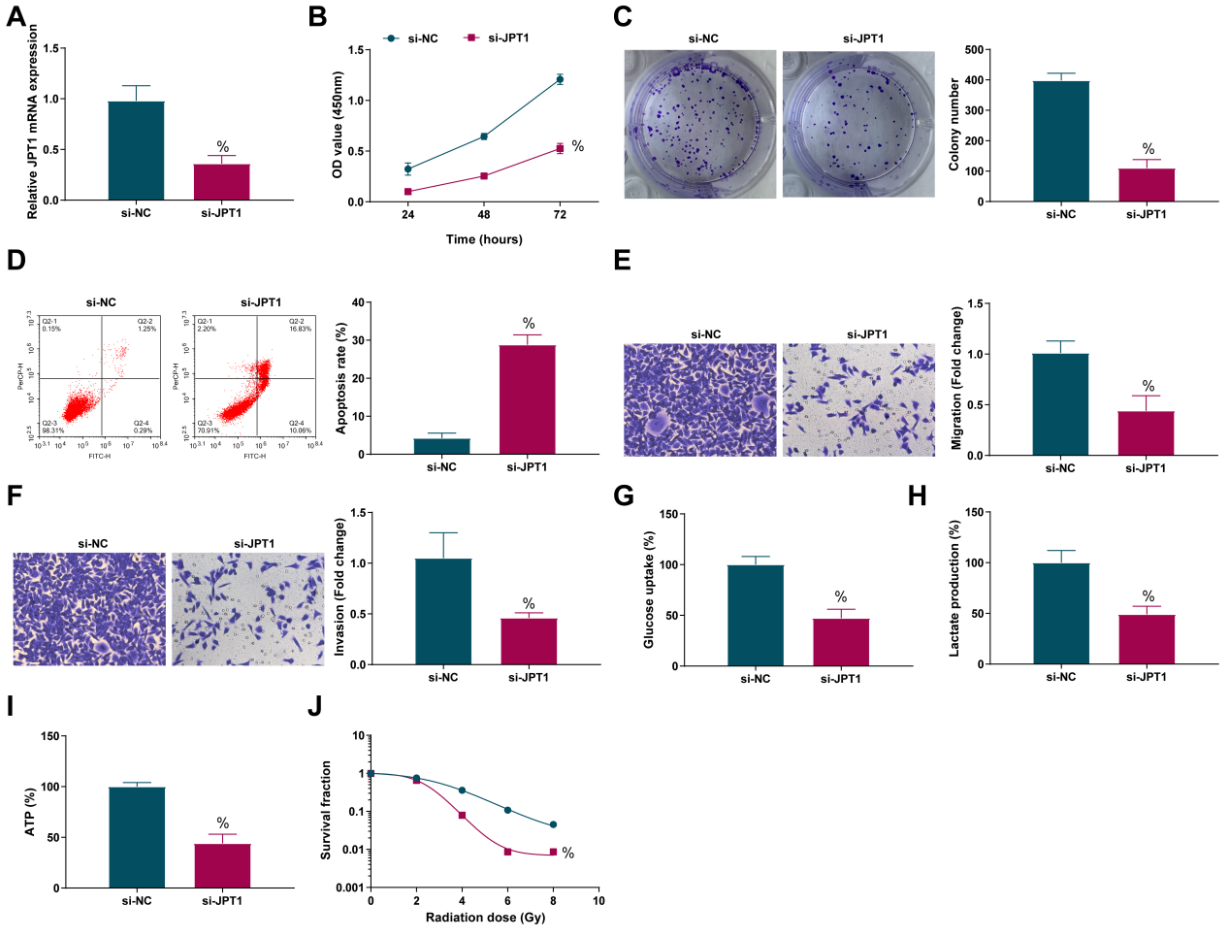

Figure 6. Inhibition of JPT1 inhibits cell growth and glycolysis, and promotes radiosensitivity *in vitro*
(**A**) circLPAR3-shRNA lentiviral transfection efficiency; (**B**) CCK-8 and (**C**) plate clone to detect cell proliferation ability after repressing circLPAR3; (**D**) Flow cytometry to detect cell apoptosis after depressing circLPAR3; (**E, F**) Transwell detection of cell migration and invasion abilities after restrained circLPAR3; (**G–I**) Glucose uptake, lactate production and ATP metabolism analysis of cell glycolysis; (**J**) Under radiation (0, 2, 4, 6 and 8 Gy) irradiation, colony formation assay to analyze the survival of the transduced cells. N=3; The data in the figure were all measurement data, the manifestation of which was as mean ± S.D. %*vs*. the si-NC, $P<0.05$.

glycolysis is an effective treatment to prevent PCa. Numerous studies have clarified that circRNA is available to impact the glycolysis of cancer cells. For instance, circDENND4C accelerates the advancement with glycolysis of colorectal cancer cells *via* the miR-760/GLUT1 axis (Zhang *et al*., 2020). Circ_0057553/miR-515-5p controls PCa cell advancement with glycolysis *via* targeting YES1 (Zhang *et al*., 2020). In the meantime, in this study, it was discovered that circLPAR3 expression was also elevated in PCa cells. Knockdown of circLPAR3 clearly repressed cell advancement with glycolysis. Additionally, at the clinical level, radiation therapy is the most familiar and ideal cure way for PCa (Miszczyk *et al*., 2021). However, because cancer cells have different repair abilities after radiation, radioresistance has always been a challenge for cure (Ihara *et al*., 2019). It came out that the silencing of circLPAR3 clearly enhanced radiosensitivity.

Former studies have manifested that circRNA is available to be applied as a competitive endogenous RNA (ceRNA) of miRNA to adsorb miRNA to modulate mRNA gene expression (Shu *et al*., 2019). For instance, circ CCNB2 knockdown depresses autophagy of PCa cells *via* targeting the miR-30b-5p/KIF18A axis and makes PCa sensitive to radiation (Cai *et al*., 2020). In this study, it was confirmed that miR-513b-5p was a circLPAR3's target. Former studies have testified that miR-513b-5p is crucial in various human cancers, like embryonic testicular cancer (Wang *et al*., 2017), breast cancer (Muti *et al*., 2018) and pancreatic cancer (Li *et al*., 2021). In the research, it was discovered the reduction of miR-513b-5p in PCa; Up-regulated miR-513b-5p repressed cell progression with glycolysis but enhanced radiosensitivity *in vitro*. As far as we know, this is the first study on miR-513b-5p in PCa.

Next, it was further figured out the downstream target genes of miR-513-5p. JPT1 is a protein-coding gene that impacts cell apoptosis and signal transduction (Bateman *et al*., 2020). A previous study has clarified that JPT1 is linked with the progression of PCa (Cheng *et al*., 2021). However, since there is very little research on JPT1, further studies are required to figure out the molecular mechanism of its action. In the research, it was discovered that JPT1 mRNA was clearly up-regulated in PCa. Moreover, elevated JPT1 reversed the effect of knocking down circLPAR3 or up-regulating miR-513b-5p on PCa cells, facilitating the advancement with glycolysis, but repressing radiosensitivity. All in all, JPT1 involves in circLPAR3/miR-513b-5p axis-regulated PCa cell growth and metastasis.

However, this research still has some limitations. First, owing to limited conditions, the sample size an-

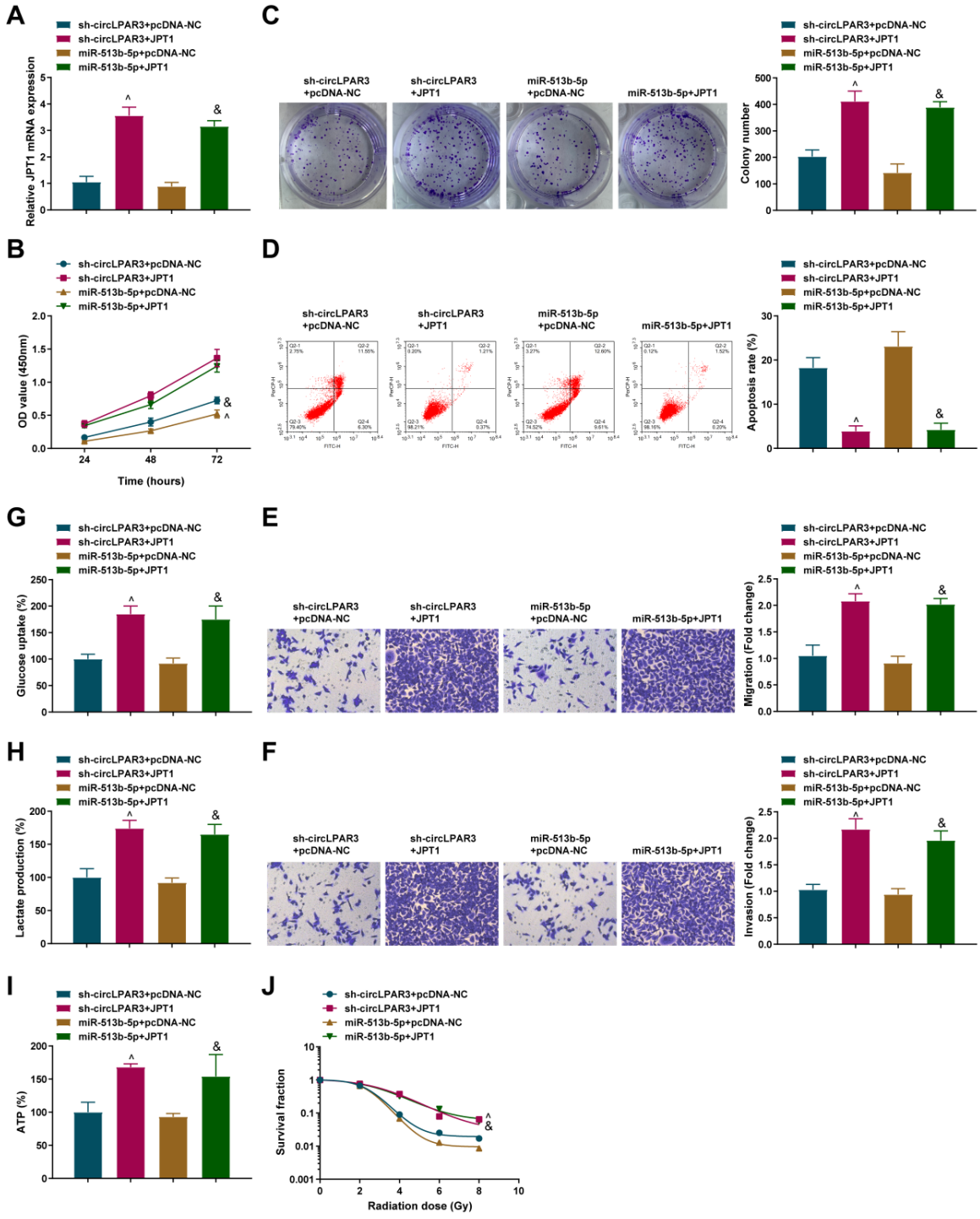

Figure 7. Overexpression of JPT1 reversed the role of downregulated circLPAR3 or upregulated miR-513b-5p on cancer cell growth. (**A**) qPCR to detect transfection efficiency; (**B**) CCK-8 method and (**C**) plate clone to detect cell proliferation. (**D**) Flow cytometry to detect cell apoptosis; (**E**) Transwell method to detect cell migration and invasion. (**F–I**) Glucose uptake, lactic acid production and ATP metabolism analysis of cellular glycolysis; (**J**) Under different doses of radiation, the survival rate of PCa cells detected by colony formation experiments. N=3; The data in the figure were all measurement data, the manifestation of which was as mean ± S.D. ^*vs.* the sh-circLPAR3+pcDNA-NC, $P<0.05$; &*vs.* the miR-513b-5p+pcDNA-NC, $P<0.05$.

alyzed is limited. Secondly, *in vivo* animal experiments were not further conducted to verify the influence of the circLPAR3/miR-513b-5p/JPT1 axis on PCa *in vivo*. Finally, further exploration of the downstream target genes of JPT1 was not implemented. We hope that these issues can be further figured out in later studies.

CONCLUSION

In conclusion, the research has discovered a new mechanism of action of circRNA in PCa. It is found that circLPAR3 performs as a sponge of miR-513b-5p in PCa to restrain PCa cell glycolysis and accelerate radiosensitivity, while upregulation of JPT1 reverses this ef-

fect. The results indicate the circLPAR3/miR-513b-5p/JPT1 axis is supposed to be a latent prognostic and therapeutic target to improve the diagnosis and treatment of PCa.

Declarations

Acknowledgments. Not applicable.

Declaration of Conflicting Interests. The author(s) declared no potential conflicts of interest with respect to the research, authorship, and/or publication of this article.

REFERENCES

Bateman NW, Teng PN, Hope E, Hood BL, Oliver J, Ao W, Zhou M, Wang G, Tommarello D, Wilson K, Litzy T, Conrads KA, Hamilton CA, Darcy KM, Casablanca Y, Maxwell GL, Bae-Jump V, Conrads TP (2020) Jupiter microtubule-associated homolog 1 (JPT1): A predictive and pharmacodynamic biomarker of metformin response in endometrial cancers. *Cancer Med* **9**: 1092–1103. https://doi.org/10.1002/cam4.2729

Cai F, Li J, Zhang J, Huang S (2022) Knockdown of Circ_CCNB2 sensitizes prostate cancer to radiation through repressing autophagy by the miR-30b-5p/KIF18A axis. *Cancer Biother Radiopharm* **37**: 480–493. https://doi.org/10.1089/cbr.2019.3538

Cai Y, Wu Q, Liu Y, Wang J (2020) AZIN1-AS1, a novel oncogenic lncrna, promotes the progression of non-small cell lung cancer by regulating MiR-513b-5p and DUSP11. *Onco Targets Ther* **13**: 9667–9678. https://doi.org/10.2147/ott.s261497

Chen JY, Xu LF, Hu HL, Wen YQ, Chen D, Liu WH (2020) MiRNA-215-5p alle*via*tes the metastasis of prostate cancer by targeting PGK1. *Eur Rev Med Pharmacol Sci* **24**: 639–646. https://doi.org/10.26355/eurrev_202001_20040

Cheng Y, Xiong HY, Li YM, Zuo HR, Liu Y, Liao GL (2021) LncRNA HOXA11-AS promotes cell growth by sponging miR-24-3p to regulate JPT1 in prostate cancer. *Eur Rev Med Pharmacol Sci* **25**: 4668–4677. https://doi.org/10.26355/eurrev_202107_26377

Du S, Zhang P, Ren W, Yang F, Du C (2020) Circ-ZNF609 accelerates the radioresistance of prostate cancer cells by promoting the glycolytic metabolism through miR-501-3p/HK2 axis. *Cancer Manag Res* **12**: 7487–7499. https://doi.org/10.2147/cmar.s257441

Dyshlovoy SA, Pelageev DN, Hauschild J, Sabutskii YE, Khmelevskaya EA, Krisp C, Kaune M, Venz S, Borisova KL, Busenbender T, Denisenko VA, Schlüter H, Bokemeyer C, Graefen M, Polonik SG, Anufriev VP, Amsberg GV (2020) Inspired by sea urchins: warburg effect mediated selectivity of novel synthetic non-glycoside 1,4-naphthoquinone-6s-glucose conjugates in prostate cancer. *Mar Drugs* **18**. https://doi.org/10.3390/md18050251

Ghafouri-Fard S, Shoorei H, Taheri M (2020) Role of microRNAs in the development, prognosis and therapeutic response of patients with prostate cancer. *Gene* **759**: 144995. https://doi.org/10.1016/j.gene.2020.144995

Ihara M, Ashizawa K, Shichijo K, Kudo T (2019) Expression of the DNA-dependent protein kinase catalytic subunit is associated with the radiosensitivity of human thyroid cancer cell lines. *J Radiat Res* **60**: 171–177. https://doi.org/10.1093/jrr/rry097

Jin W, Liang Y, Li S, Lin G, Liang H, Zhang Z, Zhang W, Nie R (2021) MiR-513b-5p represses autophagy during the malignant progression of hepatocellular carcinoma by targeting PIK3R3. *Aging (Albany NY)* **13**: 16072–16087. https://doi.org/10.18632/aging.203135

Kong Z, Wan X, Zhang Y, Zhang P, Zhang Y, Zhang X, Qi X, Wu H, Huang J, Li Y (2017) Androgen-responsive circular RNA circSMARCA5 is up-regulated and promotes cell proliferation in prostate cancer. *Biochem Biophys Res Commun* **493**: 1217–1223. https://doi.org/10.1016/j.bbrc.2017.07.162

Li S, Zhang Q, Liu W, Zhao C (2021) Silencing of FTX suppresses pancreatic cancer cell proliferation and invasion by upregulating miR-513b-5p. *BMC Cancer* **21**: 290. https://doi.org/10.1186/s12885-021-07975-6

Li XR, Zhou KQ, Yin Z, Gao YL, Yang X (2020) Knockdown of FBP1 enhances radiosensitivity in prostate cancer cells by activating autophagy. *Neoplasma* **67**: 982–991. https://doi.org/10.4149/neo_2020_190807N728

Lin W, Ye H, You K, Chen L (2020) Up-regulation of circ_LARP4 suppresses cell proliferation and migration in ovarian cancer by regulating miR-513b-5p/LARP4 axis. *Cancer Cell Int* **20**: 5. https://doi.org/10.1186/s12935-019-1071-z

Liu T, Ye P, Ye Y, Lu S, Han B (2020) Circular RNA hsa_circRNA_002178 silencing retards breast cancer progression *via* microRNA-328-3p-mediated inhibition of COL1A1. *J Cell Mol Med* **24**: 2189–2201. https://doi.org/10.1111/jcmm.14875

Miszczyk J, Przydacz M, Zembrzuski M, Chłosta PL (2021) Investigation of chromosome 1 aberrations in the lymphocytes of prostate cancer and benign prostatic hyperplasia patients by fluorescence in situ hybridization. *Cancer Manag Res* **13**: 4291–4298. https://doi.org/10.2147/cmar.s293249

Muti P, Donzelli S, Sacconi A, Hossain A, Ganci F, Frixa T, Sieri S, Krogh V, Berrino F, Biagioni F, Strano S, Beyene J, Yarden Y, Blandino G (2018) MiRNA-513a-5p inhibits progesterone receptor expression and constitutes a risk factor for breast cancer: the hOrmone and Diet in the ETiology of breast cancer prospective study. *Carcinogenesis* **39**: 98–108. https://doi.org/10.1093/carcin/bgx126

Nayak B, Khan N, Garg H, Rustagi Y, Singh P, Seth A, Dinda AK, Kaushal S (2020) Role of miRNA-182 and miRNA-187 as potential biomarkers in prostate cancer and its correlation with the staging of prostate cancer. *Int Braz J Urol* **46**: 614–623. https://doi.org/10.1590/s1677-5538.ibju.2019.0409

Porzycki P, Ciszkowicz E, Semik M, Tyrka M (2018) Combination of three miRNA (miR-141, miR-21, and miR-375) as potential diagnostic tool for prostate cancer recognition. *Int Urol Nephrol* **50**: 1619–1626. https://doi.org/10.1007/s11255-018-1938-2

Shi J, Liu C, Chen C, Guo K, Tang Z, Luo Y, Chen L, Su Y, Xu K (2020) Circular RNA circMBOAT2 promotes prostate cancer progression *via* a miR-1271-5p/mTOR axis. *Aging (Albany NY)* **12**: 13255-13280. https://doi.org/10.18632/aging.103432

Shi Y, Fang N, Li Y, Guo Z, Jiang W, He Y, Ma Z, Chen Y (2020) Circular RNA LPAR3 sponges microRNA-198 to facilitate esophageal cancer migration, invasion, and metastasis. *Cancer Sci* **111**: 2824–2836. https://doi.org/10.1111/cas.14511

Shu X, Cheng L, Dong Z, Shu S (2019) Identification of circular RNA-associated competing endogenous RNA network in the development of cleft palate. *J Cell Biochem* **120**: 16062–16074. https://doi.org/10.1002/jcb.28888

Suer I, Guzel E, Karatas OF, Creighton CJ, Ittmann M, Ozen M (2019) MicroRNAs as prognostic markers in prostate cancer. *Prostate* **79**: 265–271. https://doi.org/10.1002/pros.23731

Wang C, Tao W, Ni S, Chen Q (2019) SENP1 interacts with HIF1α to regulate glycolysis of prostatic carcinoma cells. *Int J Biol Sci* **15**: 395–403. https://doi.org/10.7150/ijbs.27256

Wang J, Li X, Xiao Z, Wang Y, Han Y, Li J, Zhu W, Leng Q, Wen Y, Wen X (2019) MicroRNA-488 inhibits proliferation and glycolysis in human prostate cancer cells by regulating PFKFB3. *FEBS Open Bio* **9**: 1798–17807. https://doi.org/10.1002/2211-5463.12718

Wang X, Zhang X, Wang G, Wang L, Lin Y, Sun F (2017) Hsa-miR-513b-5p suppresses cell proliferation and promotes P53 expression by targeting IRF2 in testicular embryonal carcinoma cells. *Gene* **626**: 344–353. https://doi.org/10.1016/j.gene.2017.05.033

Weng XD, Yan T, Liu CL (2020) Circular RNA_LARP4 inhibits cell migration and invasion of prostate cancer by targeting FOXO3A. *Eur Rev Med Pharmacol Sci* **24**: 5303–5309. https://doi.org/10.26355/eurrev_202005_21312

Wu QQ, Zheng B, Weng GB, Yang HM, Ren Y, Weng XJ, Zhang SW, Zhu WZ (2019) Downregulated NOX4 underlies a novel inhibitory role of microRNA-137 in prostate cancer. *J Cell Biochem* **120**: 10215–10227. https://doi.org/10.1002/jcb.28306

Xia L, Sun J, Xie S, Chi C, Zhu Y, Pan J, Dong B, Huang Y, Xia W, Sha J, Xue W (2020) PRKAR2B-HIF-1α loop promotes aerobic glycolysis and tumour growth in prostate cancer. *Cell Prolif* **53**: e12918. https://doi.org/10.1111/cpr.12918

Xu F, Ni M, Li J, Cheng J, Zhao H, Zhao J, Huang S, Wu X (2020) Circ0004390 promotes cell proliferation through sponging miR-198 in ovarian cancer. *Biochem Biophys Res Commun* **526**: 14–20. https://doi.org/10.1016/j.bbrc.2020.03.024

Yuan Y, Chen X, Huang E (2019) Upregulation of circular RNA Itchy E3 ubiquitin protein ligase inhibits cell proliferation and promotes cell apoptosis through targeting MiR-197 in prostate cancer. *Technol Cancer Res Treat* **18**: 1533033819886867. https://doi.org/10.1177/1533033819886867

Zhang Y, Shi Z, Li Z, Wang X, Zheng P, Li H (2020) Circ_0057553/miR-515-5p regulates prostate cancer cell proliferation, apoptosis, migration, invasion and aerobic glycolysis by targeting YES1. *Onco Targets Ther* **13**: 11289–11299. https://doi.org/10.2147/ott.s272294

Zhang ZJ, Zhang YH, Qin XJ, Wang YX, Fu J (2020) Circular RNA circDENND4C facilitates proliferation, migration and glycolysis of colorectal cancer cells through miR-760/GLUT1 axis. *Eur Rev Med Pharmacol Sci* **24**: 2387–2400. https://doi.org/10.26355/eurrev_202003_20506

Zhang ZJ, Zhang YH, Qin XJ, Wang YX, Fu J (2020) Circular RNA circMDM2 accelerates the glycolysis of oral squamous cell carcinoma by targeting miR-532-3p/HK2. *J Cell Mol Med* **24**: 7531–7537. https://doi.org/10.1111/jcmm.15380

Zhou K, Wei Y, Li X, Yang X (2021) MiR-223-3p targets FOXO3a to inhibit radiosensitivity in prostate cancer by activating glycolysis. *Life Sci* **282**: 119798. https://doi.org/10.1016/j.lfs.2021.119798.